

Human adenylate kinase 2 deficiency causes a profound hematopoietic defect associated with sensorineural deafness

Chantal Lagresle-Peyrou^{1–3,18}, Emmanuelle M Six^{1,2,18}, Capucine Picard^{1,2,4,5}, Frédéric Rieux-Laucat^{1,2}, Vincent Michel⁶, Andrea Ditadi^{1,2}, Corinne Demerens-de Chappedelaine^{1,2}, Estelle Morillon^{1,2}, Françoise Valensi¹, Karen L Simon-Stoos⁷, James C Mullikin⁸, Lenora M Noroski⁹, Céline Besse¹⁰, Nicolas M Wulffraat¹¹, Alina Ferster¹², Manuel M Abecasis¹³, Fabien Calvo¹⁴, Christine Petit^{6,15}, Fabio Candotti⁸, Laurent Abel^{2,5,19}, Alain Fischer^{1,2,16,19} & Marina Cavazzana-Calvo^{1,2,17}

Reticular dysgenesis is an autosomal recessive form of human severe combined immunodeficiency characterized by an early differentiation arrest in the myeloid lineage and impaired lymphoid maturation. In addition, affected newborns have bilateral sensorineural deafness. Here we identify biallelic mutations in AK2 (adenylate kinase 2) in seven individuals affected with reticular dysgenesis. These mutations result in absent or strongly decreased protein expression. We then demonstrate that restoration of AK2 expression in the bone marrow cells of individuals with reticular dysgenesis overcomes the neutrophil differentiation arrest, underlining its specific requirement in the development of a restricted set of hematopoietic lineages. Last, we establish that AK2 is specifically expressed in the stria vascularis region of the inner ear, which provides an explanation of the sensorineural deafness in these individuals. These results identify a previously unknown mechanism involved in regulation of hematopoietic cell differentiation and in one of the most severe human immunodeficiency syndromes.

The term ‘reticular dysgenesis’ was coined in 1959 by de Vall and Seyneheve¹ and relates to the histological findings in primary and

secondary lymphohematopoietic organs, where the scarcity of cells highlights the prominent reticular tissue framework. The lack of polymorphonuclear neutrophils (PMNs) in affected individuals is responsible for the occurrence of severe infections earlier than is usually observed in other forms of SCID^{2,3}. Reticular dysgenesis-associated neutropenia is characterized by lack of responsiveness to granulocyte-colony stimulating factor (G-CSF)⁴. The only available treatment for reticular dysgenesis is allogeneic hematopoietic stem cell transplantation (HSCT), which formally demonstrates that the inherited defect is cellular and not microenvironmental⁵.

In order to determine the molecular genetic basis of reticular dysgenesis, we took advantage of three separate consanguineous kindreds (family A, B and C, **Fig. 1a**). A genome-wide linkage scan generated a significant, multipoint lod score of 4.47 in a single region located on the short arm of chromosome 1 (1p31–p34). We then refined the map by genotyping 17 additional microsatellite markers in this region. The 90% confidence interval (CI) of the region of interest covered ~4 Mb, stretching from 30.89 to 34.79 Mb (**Fig. 1b**). Notably, two subjects originating from the same geographical area (P1 and P2) were found to be homozygous for the same haplotype in the region between 32.8 and 34.79 Mb (including 18 SNPs and 8 microsatellite markers), which strongly suggested a founder effect in these two

¹Research Laboratory on Normal and Pathologic Development of the Immune System, U768, Institut National de la Santé et de la Recherche Médicale (INSERM), 75015 Paris, France. ²Université Paris Descartes, Faculté de Médecine, IFR94, 75015 Paris, France. ³Laboratoire d'Immunologie Cellulaire et Immunopathologie de l'Ecole Pratique des Hautes Etudes and UMR 7151 Centre National de la Recherche Scientifique Université Paris 7, 75015 Paris, France. ⁴Centre d'Étude des Déficits Immunitaires, Assistance Publique-Hôpitaux de Paris, Hôpital Necker-Enfants Malades, 75015 Paris, France. ⁵Laboratory of Human Genetics of Infectious Diseases, U550, Institut National de la Santé et de la Recherche Médicale, 75015 Paris, France. ⁶Unité de Génétique et Physiologie de l'Audition, UMRS587 INSERM-Université Paris VI, Institut Pasteur, 75015 Paris, France. ⁷Genetics and Molecular Biology Branch, National Human Genome Research Institute, National Institutes of Health, Bethesda, Maryland 20892, USA. ⁸Genome Technology Branch, National Human Genome Research Institute, National Institutes of Health, Bethesda, Maryland 20892, USA. ⁹Division of Allergy and Immunology, Department of Pediatrics, Baylor College of Medicine, Houston, Texas 77030, USA. ¹⁰Centre National de Génotypage, Institut Génétique, Commissariat à l'Energie Atomique, 91000 Evry, France. ¹¹Department of Immunology/BMT, Wilhelmina Children's Hospital, Utrecht Medical Center, 3584 CX Utrecht, The Netherlands. ¹²Pediatric Hemato-Oncology Unit, Children's University Hospital Reine Fabiola, 1020 Brussels, Belgium. ¹³Bone Marrow Transplantation Unit, Portuguese Institute of Oncology Francisco Gentil, 1099-023 Lisboa, Portugal. ¹⁴Clinical Investigation Center, INSERM U716, AP-HP, University Paris 7, Hôpital Saint-Louis, 75015 Paris, France. ¹⁵Collège de France, 11 place Marcellin Berthelot, 75015 Paris, France. ¹⁶AP-HP, Hôpital Necker-Enfants Malades, Service d'Immunologie et d'Hématologie Pédiatrique, 75015 Paris, France. ¹⁷AP-HP, Hôpital Necker-Enfants Malades, Département de Biothérapie, 75015 Paris, France. ¹⁸These authors contributed equally to this work. ¹⁹These authors contributed equally to this work. Correspondence should be addressed to M.C.-C. (m.cavazzana@nck.aphp.fr).

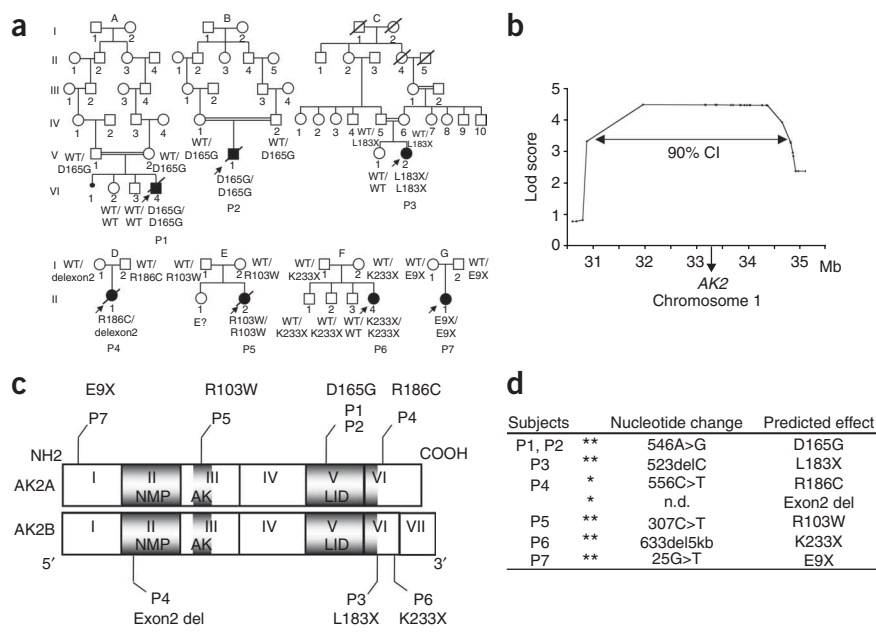


Figure 1 *AK2* gene mutations in seven individuals with reticular dysgenesis. **(a)** Genealogical trees for seven families with children suffering from reticular dysgenesis (indicated by filled symbols). Diagonal bars indicate deceased individuals. Double horizontal bars indicate consanguineous marriages. *AK2* mutations are indicated for each affected child and parent. WT, wild-type allele of the *AK2* gene. E?, no material available. **(b)** Genome-wide linkage analysis. Multipoint lod scores are plotted along the 1p30–p35 region of chromosome 1. **(c)** Location of *AK2* mutations in subjects with reticular dysgenesis. Diagrammatic representation of the *AK2A*- and *AK2B*-encoding regions from exon 1 to 7. The *AK2A* isoform includes the first six exons, whereas *AK2B* has an additional seventh exon. The corresponding protein domains are shown in dark gray: NMP binding domain (NMP), adenylate kinase domain (AK) and LID domain (LID). **(d)** Description of the *AK2* gene mutations in the seven affected individuals. In six subjects, the mutations were homozygous (***) and in one subject, they were heterozygous (*). n.d., not determined.

families and reduced the prime region of interest to ~2 Mb. We then fully sequenced the prime region of interest (**Supplementary Table 1** online). Subjects from the three consanguineous families (P1, P2 and P3) were found to be homozygous for mutations in the gene encoding adenylate kinase 2 (*AK2*). Similarly, we found *AK2* mutations in four additional individuals with reticular dysgenesis born to nonconsanguineous parents (**Fig. 1a**).

The *AK2* gene encodes two types of mRNA (expressed via an alternative splicing mechanism): *AK2A*, which has six exons, and *AK2B*, which includes an additional seventh exon located in the 3' part of the gene. *AK2A* and *AK2B* encode, respectively, a 239-amino-acid and a 232-amino-acid protein⁶.

Homozygous mutations were prevalent among the defects found in the seven affected individuals analyzed (**Fig. 1c**): three individuals (P1, P2 and P5) showed homozygous missense mutations of highly conserved amino acid residues (**Supplementary Fig. 1** online), two individuals (P3 and P6) carried a homozygous deletion (1 bp and ~5 kb, respectively) that generated a premature stop codon, and one case (P7) carried a homozygous nonsense mutation. P4 was found to be a compound heterozygote with a missense mutation and an exon 2 deletion (**Fig. 1c,d**). All mutations affect different key domains of the *AK2* protein (**Fig. 1c**) and are thus expected to severely hamper its stability and/or function. In all cases, the parents were found to be heterozygous for the mutated *AK2* allele and the healthy siblings that we tested were heterozygous or homozygous for the wild-type allele (**Fig. 1a**).

AK2 is expressed in the mitochondrial intermembrane space in a variety of tissues, such as the liver, kidney, spleen and heart⁶. We assessed the expression of the *AK2* gene in fibroblasts (either primary cultures or SV40-transformed cells) obtained from subjects P1, P3, P5 and P6 and in a B-EBV cell line from subject P2. Using protein blot analysis, we did not detect any *AK2* protein in the fibroblasts from P1, P3 and P6 (**Fig. 2a**). *AK2* protein was detected in the B-EBV cell line and in fibroblasts derived from P2 and P5, respectively, but at markedly lower levels than in control cells (**Fig. 2a**). In contrast to the *AK2* protein, *AK2* mRNA was detected by RT-PCR at levels comparable to those found in control cell lines in all samples analyzed (**Fig. 2b**). These data

strongly suggest that reticular dysgenesis results from loss-of-function mutations in the *AK2* gene.

Analysis of the immunological characteristics of individuals with reticular dysgenesis showed that the profound neutropenia was invariably associated with an equally profound T and natural killer (NK) cell lymphopenia, whereas the B cell lineage was variably affected (**Table 1**). The circulating monocyte count was normal or above normal, and red blood cell and platelet counts were normal or slightly diminished, as also observed previously⁷. Morphological examination of the bone marrow revealed a profound block in granulopoiesis, with no detectable cells beyond the myelocyte stage, thus indicating that reticular dysgenesis corresponds to a selective developmental arrest along T, NK lymphoid and granulocytic myeloid pathways. In

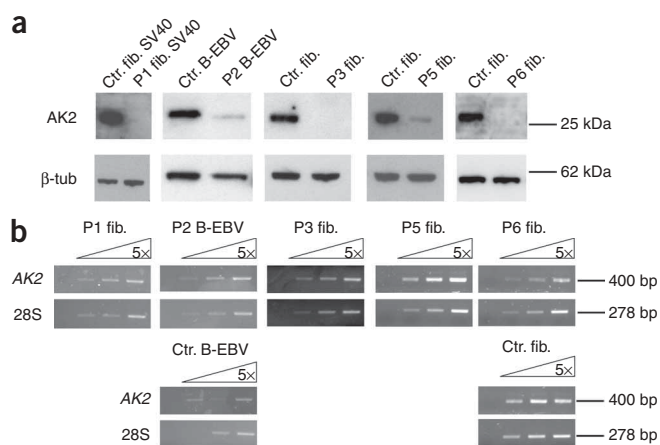


Figure 2 Gene and protein expression analysis of *AK2* in cell lines derived from individuals with reticular dysgenesis. **(a)** Protein blot analysis of *AK2* expression. Lysates from fibroblast (Fib) or B-EBV cell lines derived from affected individuals were immunoblotted with an antibody to *AK2* and with antibody to β -tubulin as a loading control. **(b)** RT-PCR analysis of *AK2* expression. cDNA prepared from fibroblast or B-EBV cell lines derived from affected individuals was analyzed by RT-PCR using fivefold serial dilution. The cDNA input was normalized against 28S-rRNA gene expression.

Table 1 Hematological and immunological characteristics of subjects with reticular dysgenesis

Subject	P1	P2	P3	P4	P5	P6	P7	Age-matched control values 0–1 month
WBCs (10^{-9} cells/l)	0.5	1.63	0.39	1.8	1.4	0.3	0.85	7.20–18.00
Lymphocytes (10^{-9} cells/l)	0.30	0.67	0.26	0.9	0.8	0.07	0.35	3.40–7.60
T lymphocytes (10^{-9} cells/l)	0.27	0.04	0.01	0.09	0.1	0.001	0.02	2.50–5.50
CD4 ⁺ T cells (10^{-9} cells/l)	0.10	0.001	0.004	n.a.	0.09	0	0.01	1.60–4.00
CD8 ⁺ T cells (10^{-9} cells/l)	0.03	0.04	0.004	n.a.	0	0	0.006	0.56–1.70
B lymphocytes (10^{-9} cells/l)	0	0.556	0.165	n.a.	0.5	0	0.3	0.3–2.00
NK cells (10^{-9} cells/l)	0.017	0.053	0.008	0.09	0.056	n.a.	0.03	0.17–1.10
PMNs (10^{-9} cells/l)	0	0.03	0	0.15	0.15	0	0.10	1.50–8.50
Monocytes (10^{-9} cells/l)	0.2	0.555	0.15	0.55	0.4	0.11	0.4	0.20–1.00
Platelets (10^{-9} cells/l)	275	62	100	442	300	172	200	175–500
Hemoglobin (g/dl)	8	15	10	15.5	12	11.5	14.6	14.0–17.0

WBC, white blood cells; PMN, polymorphonuclear cells; NK, natural killer cells; n.a., not available. All subjects were diagnosed within the first month of life.

semisolid medium, CD34⁺ cells isolated from the bone marrow of P2 did not generate granulocytic colonies, and only a few myeloblasts and erythroblasts were observed before and after culture (**Supplementary Fig. 2a** online). In subject P2, after CD34⁺ cells were cultured in the presence of SCF, FLT-3L and GM-CSF or G-CSF cytokines, CD15⁺ CD11b⁺ neutrophil cell counts were two and four times lower, respectively, than in control cord blood cell cultures (**Supplementary Fig. 2b**), suggesting a potential role for AK2 in the G-CSF receptor-mediated myeloid differentiation. This is in agreement with the G-CSF refractory neutropenia observed in affected individuals.

As a first step toward elucidating the function of AK2 in hematopoiesis, we carried out an RT-PCR AK2 gene expression profile analysis, which showed AK2 upregulation in the various hematopoietic subsets as compared to a fibroblast cell line (**Supplementary Fig. 3** online). These results fit with a differential and specific role of AK2 in different cell types.

In order to prove unequivocally that AK2 mutations were responsible for the profound neutropenia, we set out to restore myeloid differentiation *in vitro* by transducing bone marrow CD34⁺ cells from affected individuals with a lentivirus encoding cDNA of both

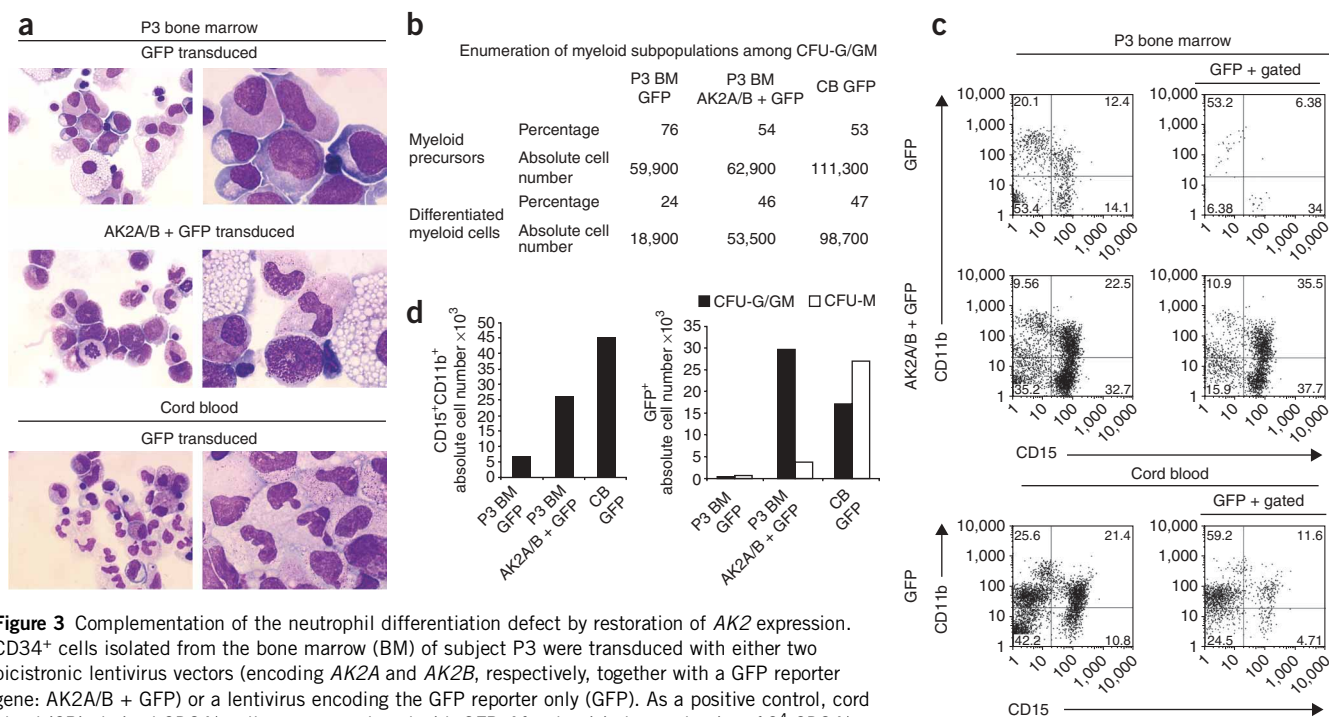


Figure 3 Complementation of the neutrophil differentiation defect by restoration of AK2 expression. CD34⁺ cells isolated from the bone marrow (BM) of subject P3 were transduced with either two bicistronic lentivirus vectors (encoding AK2A and AK2B, respectively, together with a GFP reporter gene: AK2A/B + GFP) or a lentivirus encoding the GFP reporter only (GFP). As a positive control, cord blood (CB)-derived CD34⁺ cells were transduced with GFP. After lentiviral transduction, 10⁴ CD34⁺ cells from the bone marrow of P3 were seeded in semisolid medium for each condition, corresponding to 500 complemented cells (based on a transduction efficiency of 5%). As a control, 500 CD34⁺ cord blood cells were seeded in semisolid medium (transduction efficiency of 35%). (a) After 13 days, CFU-G/GM colonies were collected and cytospin preparations of each condition (P3 BM GFP; P3 BM AK2A/B + GFP; CB GFP) were analyzed by May-Grunwald-Giemsa staining. Representative pictures of various stages of neutrophil maturation are shown at magnifications of ×50 (left panel) or ×100 (right panel). (b) Enumeration of myeloid subpopulations among CFU-G/GM colonies. Myeloid precursors (blasts, myeloblasts and promyelocytes) and differentiated myeloid cells (myelocytes, metamyelocytes and granulocytes) are represented in percentage and in absolute cell numbers. (c) Representative flow cytometry analysis of CD15 and CD11b expression in CFU-G/GM colonies (left-hand dot plots) and on transduced GFP⁺ CFU-G/GM colonies (right-hand dot plots). (d) Absolute number of double-positive CD15⁺ CD11b⁺ labeled cells are indicated for each condition (left panel). The absolute number of GFP⁺ cells isolated from the CFU-G/GM colonies and from the CFU-M colonies are indicated (right panel).

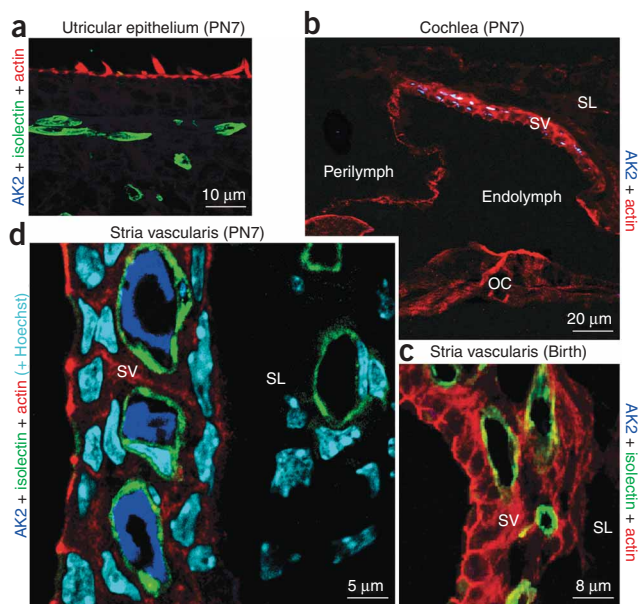


Figure 4 AK2 distribution in the mouse inner ear. (a) AK2 is not detected in the vestibular epithelium. (b) In the postnatal day 7 (PN7) cochlea, AK2 is only detected in the stria vascularis (SV). It is absent from the spiral ligament (SL) and organ of Corti (OC). (c) AK2 is not detected in the SV at birth. (d) In the PN7 SV, AK2 labeling (dark blue) is restricted to the lumen of the capillaries and terminal blood vessels, which are stained green with isolectin. Blood vessels in the spiral ligament (SL) do not contain AK2. Cell nuclei are stained in light blue by Hoechst staining.

AK2A + AK2B. Granulocyte/granulocyte-monocyte (G/GM) colonies derived from bone marrow cells of P3 and transduced with a control GFP vector were characterized by the presence of immature myeloblasts, promyelocytes, and very few mature myelocytes and polynucleated cells. In contrast, G/GM colonies derived from bone marrow cells transduced with *AK2A*, *AK2B* and GFP (*AK2A/B + GFP*) contained around 46% of mature myeloid cells, metamyelocytes and polymorphonuclear cells (Fig. 3a,b), showing the unambiguous characteristics of mature myeloid cells. These mature granulocytes were very similar to those observed in colonies cultured from control healthy cord blood cells (Fig. 3a). We confirmed these morphological observations by flow cytometry analysis (Fig. 3c) and showed that the CD15⁺ CD11b⁺ cell count was 3.7-fold higher in the *AK2A/B + GFP* condition than in the GFP condition (Fig. 3d). Furthermore, the overall count of GFP⁺AK2⁺ complemented cells in the G/GM colonies was 53-fold higher than that of GFP⁺ cells isolated from noncomplemented bone marrow cells (Fig. 3d). Restoration of neutrophil differentiation was confirmed in bone marrow cell from P6 (Supplementary Fig. 4 online). These data demonstrate that *AK2* complementation corrects the defective granulopoiesis in reticular dysgenesis.

In order to confirm the specific role of *AK2* in neutrophil differentiation, we developed a RNA interference strategy through lentiviral-mediated gene transfer of *AK2* short hairpin RNAs (shAK2), using the previously published shAK2 target sequence⁸. The downregulation of *AK2* expression in human CD34⁺ cell induced a 17- to 27-fold reduction in myeloid cells and granulocyte precursors associated with a profound arrest in neutrophil differentiation as determined by counting of CD15⁺ CD11b⁺ cells and by morphological examination (Supplementary Fig. 5 online). Conversely, no

decrease in the proliferation rate was observed in human primary fibroblasts transduced with the same *AK2* shRNA lentivirus vector (data not shown).

In order to investigate the pathogenic process underlying the hearing impairment observed in all 7 subjects with reticular dysgenesis, we analyzed the distribution of *AK2* in the mouse inner ear by immunohistolabeling. *AK2* expression could not be detected in the vestibule at any developmental stage (Fig. 4a). In contrast, assessment of the cochlea revealed an intense *AK2* staining observed uniquely in the stria vascularis at postnatal day 7 but not at birth (Fig. 4b,c). Co-immunolabeling of *AK2* and isolectin showed that *AK2* is present within the lumen of the stria vascularis capillaries (Fig. 4d), thus suggesting that it could be here functioning as an ecto-enzyme. Notably, we did not detect *AK2* in the capillaries or vessels of the adjacent connective tissue (Fig. 4d).

Our data provide evidence that recessive mutations of the human *AK2* gene are responsible for reticular dysgenesis, a very rare form of SCID characterized by a profound impairment of the lymphomyeloid compartment associated with deafness. *AK2* has a key role during development, as shown in the *Drosophila* larvae deficient for *AK2* (ref. 9). This enzyme regulates the homeostasis of cellular adenine nucleotides by converting ADP into ATP and AMP⁹ and thus may be critical in specific key subcellular or extracellular compartments. Our observations in the inner ear suggest a new function for *AK2* in the stria vascularis. Indeed, failure of the stria vascularis to produce the endocochlear potential or secrete K⁺ in the endolymph results in hearing impairment^{10,11}. Moreover, serum ADP is thought to be one of the most damaging factors for endothelial integrity, in view of its proinflammatory and thrombotic effects¹². In this respect, ecto-*AK2* in the stria vascularis microvasculature might contribute to the control of local ADP levels via reverse transphosphorylation into ATP and AMP.

In many human and murine cells, *AK2* is localized in the mitochondrial intermembrane space, suggesting a role for the protein in providing the energy required for the proliferation of hematopoietic precursors and/or in controlling cell apoptosis. With respect to the latter hypothesis, our findings are reminiscent of the results reported in another type of severe congenital neutropenia caused by HAX-1 deficiency¹³. HAX-1 is also located in the mitochondrial intermembrane space and is required to prevent apoptosis of mouse lymphocytes, granulocytes and neurons^{14,15}. *AK2* might also be involved in the regulation of apoptosis via an as-yet-unknown mechanism that may involve its release from the mitochondria, together with cytochrome *c*^{16,17}. More recently, *AK2* has been implicated in a newly identified intrinsic apoptosis pathway, where it forms a complex with FADD and caspase 10 (ref. 8). In this latter report, truncated, mislocated *AK2* products were found in the cytosol of human cells and were seen to induce apoptosis. However, our protein blot analysis did not reveal the presence of any truncated *AK2* protein. This is in agreement with the observation of a strong decrease in cell proliferation and survival as well as a block in myeloid differentiation induced by the downregulation of *AK2* expression in CD34⁺ cells. The discrepancy with the published data may be related to the usage of different cell subsets: HeLa cells in the previous study⁸ versus CD34⁺ cells in ours. Indeed, no effect on fibroblast cell survival was induced by downregulation of *AK2*. It is nevertheless possible that formation of an *AK2*-FADD-caspase 10 complex is required for commitment to the differentiation pathway of T and natural killer lymphoid cells as well as neutrophils. Indeed, the recent description of thrombocytopenia in individuals carrying mutations in the cytochrome *c* gene¹⁸ emphasizes a possible lineage-specific control of caspase activation that may not be related to the classic cell death mechanism^{19,20}. Further

investigation of the potential involvement of AK2 in regulating apoptosis in certain cell lineages is required.

We have identified mutations in human AK2 responsible for reticular dysgenesis, one of the most severe immunodeficiencies affecting both innate and adaptive immunity and associated with sensorineural deafness. These data emphasize the key role of the AK2 protein in hematopoiesis and identify a previously unknown cell-lineage restricted pathway controlling energy metabolism and/or cell growth and survival.

METHODS

Subjects. Seven families (each with one affected child) were analyzed in the present study. Three were unrelated consanguineous families (A, B, C), with two originating from Cape Verde (Western Africa) and the third from Turkey. The four other unrelated nonconsanguineous families originated from France (D), Portugal (E), The Netherlands (F) and Central America (G), respectively. All the probands were admitted to the hospital very soon after birth (from 1 day up to 1 month) because of multiple life-threatening infections. The blood cell count and the bone marrow status prompted a diagnosis of reticular dysgenesis. All of these individuals were later found to be deaf. All received an allogeneic hematopoietic stem cell transplant from one of the two parents or from phenocompatible cord blood (P6), which resulted in a cure in three (P3, P6, P7) of the seven individuals.

Genetic, sequencing and gene expression analysis. We carried out linkage analysis by homozygosity mapping²¹ of the two Cape Verde families (A, B) and the Turkish family (C) at the Centre National de Genotypage (CNG, Evry, France), and we genotyped 17 additional microsatellite markers in the region of interest by using standard methods. DNA samples from the individuals with reticular dysgenesis and their relatives were purified from peripheral blood cells by using genomic DNA Maxiprep kits (Qiagen). For target gene sequencing, we designed PCR primers for the 2-Mb region and carried out standard Sanger sequencing at the US National Institutes of Health Intramural Sequencing Center (NISC). Coding regions of AK2 (exons 1–7) were completely covered by sequencing and had very high sequence-trace quality scores. Exons 1 and 7 had double sequence coverage (four traces per subject; two forward and two reverse traces). On average, each amplicon sequenced 645 targeted bases (median, 671; mode, 700). We processed traces to detect single nucleotide and insertion/deletion (indel) variation using POLYPHRED software (version 6.11). We screened healthy individuals (100 chromosomes) for AK2 gene mutations and found none.

Cell samples and purification of human CD34⁺ cells. We harvested control human cord blood samples on delivery of full-term, healthy pregnancies at the Antoine Bécélère Hospital and the Pitié-Salpêtrière Hospital. Human bone marrow from individuals with reticular dysgenesis was collected under general anesthesia during the installation of the central line required for allogeneic bone marrow transplantation. Our study was performed with informed consent obtained from each subject or the subject's family and was approved by the Hôpital Necker independent ethics committee and the National Human Genome Research Institute institutional review board. Mononuclear cells (MNCs) and CD34⁺ cells were purified as previously described²².

For subjects P1, P3, P5 and P6, primary fibroblast cell lines were obtained from skin biopsies and fibroblasts were immortalized with SV40, as previously described²³. B-EBV cell lines (EBV-transformed B-cell lines) were generated from bone marrow samples, as described elsewhere²⁴.

In vitro myeloid differentiation assays. We evaluated the differentiation of CD34⁺ cells by clonal assay in methylcellulose (methoCult H4435), as previously described²². CD34⁺ cells were also cultured in X-Vivo 20 medium (BioWhittaker) supplemented with 10 ng/ml of stem cell factor (SCF; Amgen), and 100 ng/ml of granulocyte-macrophage colony stimulating factor (GM-CSF; Amgen) or 100 ng/ml granulocyte colony stimulating factor (G-CSF; Amgen). After 2 weeks, we harvested and analyzed cells by May-Grunwald-Giemsa staining. We also analyzed cells by flow cytometry using a combination of fluorescein isothiocyanate (FITC)-conjugated antibody to CD15 (anti-CD15,

HI98), phycoerythrin (PE)-conjugated anti-CD11b (ICRF44) and allophycocyanin (APC)-conjugated anti-CD14 (M5E2) (Becton Dickinson, BD Biosciences). Analysis was done on a FACSCalibur (BD Biosciences) using the FlowJo software.

Gene expression analysis. Total RNA was reverse transcribed using random hexamers with MultiScribe MuLV reverse transcriptase (Applied Biosystems). RT-PCR was done on each subject sample using primers specific for AK2 and 28S (Supplementary Table 2 online).

We carried out comparative real-time RT-PCR assays^{25,26} for each sample in triplicate in a final reaction volume of 50 μ l. The endogenous gene (*GAPDH*) or the gene of interest (*AK2A* or *AK2B*) were amplified using around 20 ng of cDNA, and *AK2A* (Hs00761823), *AK2B* (Hs00797700) or *GAPDH* (Hs00266705) probes labeled with a FAM, 6-carboxy-fluorescein dye (Applied Biosystems). We carried out all reactions using an ABI Prism 7900 sequence detection system (Applied Biosystems). The data were analyzed using the comparative cycle threshold method and presented as the relative change in gene expression, normalized against the calibrator sample, corresponding to a fibroblast cell line.

Protein blots. Control or reticular dysgenesis fibroblast cell lines (either primary or SV40-transformed) were lysed in a buffer (containing 20mM Tris, pH 7.9; 300 mM NaCl; 1% Nonidet P-40) supplemented with protease and phosphatase inhibitors. Cell extracts were separated by SDS-PAGE, blotted and stained with a polyclonal antibody against AK2 (H65, Santa Cruz) or with a monoclonal antibody against β tubulin (TUB2.1, Sigma). After staining with an HRP-conjugated secondary antibody, the immunoblot was developed using an ECL+ kit (Amersham).

Construction and production of the lentiviral vectors. The backbone of the replication-defective, self-inactivating pWPI lentiviral vector was provided by Addgene. The constructs were generated using *PmeI* (Ozyme) ligation of the coding sequence of human AK2A (pWPI-AK2A) or AK2B (pWPI-AK2B). For construction of AK2 short hairpin RNA (shAK2) and the negative control Scramble shRNA (shScramble), the forward and reverse primers (Supplementary Table 2) containing target sequences from AK2 corresponding to the previously published shRNA#1 (ref. 8) and from a control Scramble were cloned into the *MluI* and *ClaI* sites of the pLVTHM lentiviral vector, provided by Addgene. The latter vectors enable coexpression of GFP under the control of an EF1 α promoter. High-titer lentivirus supernatants were produced by Vectalys. Using this shAK2 lentivector, we effectively knocked down AK2 expression in cord blood-derived CD34⁺ cells as observed by quantitative RT-PCR (data not shown).

Transduction of human CD34⁺ cells. We cultured bone-marrow mononuclear cells or purified CD34⁺ cells overnight in X-vivo 20 medium supplemented with SCF (300 ng/ml), Flt3-ligand (Flt3-L, 300 ng/ml), interleukin 3 (60 ng/ml IL-3) and thrombopoietin (100 ng/ml TPO) (R&D Systems). Cells were then transferred onto culture plates coated with 50 μ g/ml of retronectin-CH296 (Takara Bio) and transduced (at 2×10^6 /ml) or not with the lentiviral supernatant (multiplicity of infection = 100) in X-vivo 20 medium supplemented with the cytokines described above and 4 μ g/ml of protamine sulfate (Choy). After an overnight culture, cells were harvested and seeded for the myeloid differentiation assay.

Immunofluorescence staining on inner ear sections. Experiments were done using 10- μ m-thick, frozen cochlear sections. We prepared cochlear sections by dissecting the temporal bones and fixing them by immersion in 4% paraformaldehyde. The samples were then decalcified in 0.5 M EDTA, immersed in 20% sucrose and frozen in OCT compound embedding medium. After blocking in 20% goat serum, the sections were incubated with the primary antibody at 4 $^{\circ}$ C for 12 h, followed by incubation with the secondary antibody (and with phalloidin and/or Hoechst dyes) for 1 h at 25 $^{\circ}$ C and, lastly, embedded in Fluorsave (Calbiochem) for confocal microscopy analysis (with the LSM510 META from Zeiss). We used the following antibodies: polyclonal anti-AK2 (Abcam), Cy5 goat anti-rabbit Ig (H+L), Cy3 goat anti-mouse Ig (H+L) (Amersham) and Alexa Fluor 488-conjugated isolectin GS-IB4 (Invitrogen).

Note: Supplementary information is available on the Nature Genetics website.

ACKNOWLEDGMENTS

We wish to thank the Antoine Bécélère Hospital and the Pitié-Salpêtrière Hospital for providing cord blood samples, the French National Genotyping Centre for contributing to the genome-wide linkage scan and P. Cherukuri and the NISC Comparative Sequencing Program (NISC, National Human Genome Research Institute, National Institutes of Health) for their help in sequencing the region of interest. We are grateful to I. André-Schmutz, S. Blanche, J.L. Casanova, J. Chinen, C. Chomienne, L. Coulombel, L. dal Cortivo, F. Le Deist, G. de Saint-Basile and J.P. de Villartay for discussions and assistance, and to all staff nurses who cared for the patients. We also thank the subjects' families for their participation. We acknowledge C. Hue, C. Martinache, J. Rouiller, C. Soudais and M.C. Stolzenberg for their technical assistance, as well as D. Fraser for his language editing review. The study was funded by the French National Institute for Health and Medical Research (INSERM), the French Institute for Rare Diseases (GIS-Institut des maladies rares), the French National Research Agency (ANR) and the Intramural Research Program of the National Human Genome Research Institute (NIH).

AUTHOR CONTRIBUTIONS

C.L.-P. and E.M.S. contributed equally to this study by performing most of the experimental work and analysis, with the assistance of C.D.-d.C. and E.M. C. Picard and F.R.-L. performed apoptotic tests on the fibroblasts, gave critical advice and comments in designing the experiments. Experiments shown in Figure 4 were performed by V.M. A.D. performed the RNA interference experiments. F.V. provided expertise in histological examination. K.L.S.-S. mapped P6 deletion and found P7 mutation. J.C.M. performed the sequencing project. C.B. performed the genome-wide linkage scan. C. Picard, L.M.N., N.M.W., A. Ferster, M.M.A. and M.C.-C. recruited and diagnosed the individuals with reticular dysgenesis and provided materials from them. F. Calvo gave critical comments in designing the experiments and helped to sequence the healthy and pathological samples. C. Petit contributed to the design of the inner ear experiments and F. Candotti designed and coordinated the sequencing project. C. Picard and L.A. performed the lod-score analysis. L.A. and A. Fischer contributed equally to this study. M.C.-C. supervised the overall project. M.C.-C., C.L.-P., E.M.S., L.A. and A. Fischer wrote the paper and added the comments from all authors.

Published online at <http://www.nature.com/naturegenetics/>

Reprints and permissions information is available online at <http://npg.nature.com/reprintsandpermissions/>

- De Vall, O. & Seyneheve, V. Reticular dysgenesis. *Lancet* **2**, 1123–1125 (1959).
- Heltzer, M.L., Paessler, M., Raffini, L., Bunin, N. & Perez, E.E. Successful haplo-identical bone marrow transplantation in a patient with reticular dysgenesis: three-year follow-up. *J. Allergy Clin. Immunol.* **120**, 950–952 (2007).
- Reubsæet, L.L., Boelens, J.J., Rademaker, C., Smal, J. & Wulffraat, N.M. Successful cord blood transplantation in a premature and dysmature neonate of 1700 g with reticular dysgenesis. *Bone Marrow Transplant.* **39**, 307–308 (2007).
- Bujan, W., Ferster, A., Sariban, E. & Friedrich, W. Effect of recombinant human granulocyte colony-stimulating factor in reticular dysgenesis. *Blood* **82**, 1684 (1993).
- Antoine, C. *et al.* Long-term survival and transplantation of haemopoietic stem cells for immunodeficiencies: report of the European experience 1968–99. *Lancet* **361**, 553–560 (2003).
- Noma, T., Song, S., Yoon, Y.S., Tanaka, S. & Nakazawa, A. cDNA cloning and tissue-specific expression of the gene encoding human adenylate kinase isozyme 2. *Biochim. Biophys. Acta* **1395**, 34–39 (1998).
- Levinsky, R.J. & Tiedeman, K. Successful bone-marrow transplantation for reticular dysgenesis. *Lancet* **1**, 671–672 (1983).
- Lee, H.J. *et al.* AK2 activates a novel apoptotic pathway through formation of a complex with FADD and caspase-10. *Nat. Cell Biol.* **9**, 1303–1310 (2007).
- Noma, T. Dynamics of nucleotide metabolism as a supporter of life phenomena. *J. Med. Invest.* **52**, 127–136 (2005).
- Cohen-Salmon, M. *et al.* Connexin30 deficiency causes intrastrial fluid-blood barrier disruption within the cochlear stria vascularis. *Proc. Natl. Acad. Sci. USA* **104**, 6229–6234 (2007).
- Wangemann, P. Supporting sensory transduction: cochlear fluid homeostasis and the endocochlear potential. *J. Physiol. (Lond.)* **576**, 11–21 (2006).
- Heine, P., Braun, N., Heilbronn, A. & Zimmermann, H. Functional characterization of rat ecto-ATPase and ecto-ATP diphosphohydrolase after heterologous expression in CHO cells. *Eur. J. Biochem.* **262**, 102–107 (1999).
- Klein, C. *et al.* HAX1 deficiency causes autosomal recessive severe congenital neutropenia (Kostmann disease). *Nat. Genet.* **39**, 86–92 (2007).
- Chao, J.R. *et al.* Hax1-mediated processing of HtrA2 by Parl allows survival of lymphocytes and neurons. *Nature* **452**, 98–102 (2008).
- Carlsson, G. & Fasth, A. Infantile genetic agranulocytosis, morbus Kostmann: presentation of six cases from the original “Kostmann family” and a review. *Acta Paediatr.* **90**, 757–764 (2001).
- Kohler, C. *et al.* Release of adenylate kinase 2 from the mitochondrial intermembrane space during apoptosis. *FEBS Lett.* **447**, 10–12 (1999).
- Munoz-Pinedo, C. *et al.* Different mitochondrial intermembrane space proteins are released during apoptosis in a manner that is coordinately initiated but can vary in duration. *Proc. Natl. Acad. Sci. USA* **103**, 11573–11578 (2006).
- Morison, I.M. *et al.* A mutation of human cytochrome c enhances the intrinsic apoptotic pathway but causes only thrombocytopenia. *Nat. Genet.* **40**, 387–389 (2008).
- Hao, Z. *et al.* Specific ablation of the apoptotic functions of cytochrome C reveals a differential requirement for cytochrome C and Apaf-1 in apoptosis. *Cell* **121**, 579–591 (2005).
- Solary, E., Giordanetto, F. & Kroemer, G. Re-examining the role of cytochrome c in cell death. *Nat. Genet.* **40**, 379–380 (2008).
- Lander, E.S. & Botstein, D. Homozygosity mapping: a way to map human recessive traits with the DNA of inbred children. *Science* **236**, 1567–1570 (1987).
- Six, E.M. *et al.* A human postnatal lymphoid progenitor capable of circulating and seeding the thymus. *J. Exp. Med.* **204**, 3085–3093 (2007).
- Nicolas, N. *et al.* A human severe combined immunodeficiency (SCID) condition with increased sensitivity to ionizing radiations and impaired V(D)J rearrangements defines a new DNA recombination/repair deficiency. *J. Exp. Med.* **188**, 627–634 (1998).
- Tosato, G. & Cohen, J.I. Generation of Epstein-Barr Virus (EBV)-immortalized B cell lines. *Curr. Protoc. Immunol.* Chapter 7, Unit 7.22 (2007).
- Peters, U.R. *et al.* Distinct expression patterns of the p53-homologue p73 in malignant and normal hematopoiesis assessed by a novel real-time reverse transcription-polymerase chain reaction assay and protein analysis. *Cancer Res.* **59**, 4233–4236 (1999).
- Bustin, S.A. Absolute quantification of mRNA using real-time reverse transcription polymerase chain reaction assays. *J. Mol. Endocrinol.* **25**, 169–193 (2000).